High-accuracy approximation of the Voigt function based on Fourier expansion of exponential multiplier

YIHONG WANG

School of Energy and Environment, Southeast University, Nanjing 210096, China

wyh@seu.edu.cn

Abstract A rapidly convergent series, based on Fourier expansion of the exponential multiplier, is presented for highly accurate approximation of the Voigt function (VF). The computational test reveals that with only the first 33 terms Fourier expansion of the exponential multiplier, this approximation provides accuracy better than 5.5383×10^{-19} in the domain of practical interest $0 < x < 40{,}000$ and $10^{-4} < y < 10^{2}$ that is needed for applications using the HITRAN molecular spectroscopic database. Compared with the typical approximation algorithms, the proposed approximation still available even if y is very small and the accuracy in the narrow band domain $0 < x < 40{,}000 \cap 10^{-10} < y < 10^{-4}$ remains high and better than 5.5385×10^{-13}.

Key words Voigt function, Fourier series, High-accuracy approximation, Boundary-free

1. Introduction

The Voigt function (VF) describes emission and absorption properties of the gas molecules in the atmosphere, and, consequently, it is widely used in many scientific disciplines[1-4]. Mathematically, the VF can be expressed in terms of the real part of the Faddeeva function or complex error function

$$w(z) = \exp(-z^2)\,\mathrm{erfc}(-iz), \tag{1}$$

where $z = x + \mathrm{i}y$ and $y > 0$. In common representation, the VF is given by the following integral

$$K(x,y) = \frac{y}{\pi}\int_{-\infty}^{\infty}\frac{\exp(-t^2)}{(x-t)^2+y^2}\,dt, \tag{2}$$

where $y = \sqrt{\ln 2}\,\alpha_L / \alpha_G$, $x = \sqrt{\ln 2}\,(v - v_0)/\alpha_G$, v is the frequency spanning from the line center v_0, α_L and α_G are Lorentz and Doppler HWHM, respectively.

Applying the Fourier transform, the Eq. (2) can be rewritten in the following form[45]

$$K(x,y) = \frac{1}{\sqrt{\pi}}\int_0^{\infty}\exp\left(-\frac{1}{4}t^2\right)\exp(-yt)\cos(xt)\,dt. \tag{3}$$

None of the integrals above have analytical solutions, thus many modern "state-of-the art" algorithms for evaluating the VF utilizing sophisticated numerical techniques have been discussed in numerous papers. An efficient algorithm on the basis of a modified Humlicek algorithm[6] was developed by Wells[7] with relative error chosen between 10^{-2} and 10^{-5}. Although the Wells algorithm is sufficient for the most practical tasks, the more accurate calculation of the VF may also be required.

Recently, Abrarov et al. [8-10] proposed two similar algorithms based on exponential series approximation for the rapid and high-accuracy calculation of the VF. Abrarov algorithm I[8-9] which based on Fourier expansion of the exponential multiplier is more accurate than 10^{-9} in the Humlicek regions 3 and 4[6]. Abrarov algorithm II[10] which based on rational approximation of the exponential multiplier provides accuracy better than 10^{-9} over a wide domain of practical interest for applications using the HITRAN molecular spectroscopic database. However

the accuracy of Abrarov algorithm I or II deteriorates further with decreasing y. Different approaches have been implemented to overcome this problem[]. For example, the Chiarella and Reichel approximation (equation (15) in [11]), the Weideman's rational approximation (equation (38-I) in [12]), the exponential series approximation (equation (14) in [13]) and the rational approximation (equation (14) in [10]) that provide highly accurate and rapid calculation for the VF within narrow band domain $0 \le x \le 15$ and $10^{-6} \le y \le 15$. However the accuracy of these algorithms deteriorates significantly while y is small than 10^{-6}. Abrarov and Quine[14] presented two approximations for the VF with small y ($y \le 10^{-6}$), however these two approximations need to calculate Dawson's integral which has no analytical solution. Therefore, The highly accurate and simultaneously rapid computation of VF at $0 < y << 1$ still remains problematic[15] and the high-accuracy approximation with boundary-free may also be required.

In this work we propose a new approximation for the VF based on the Fourier expansion of the exponential multiplier for efficient computation and the availability of the algorithm over a wide domain ($10^{-4} \le x \le 40{,}000$ and $10^{-10} \le y \le 10^{2}$) is verified by computational test. This algorithm is based on elementary functions that are freely available in a standard library of most programming languages. We applied MATLAB R2014a supporting array programming features. A typical desktop computer Intel(R) Quad CPU with RAM 4.00 GB was utilized.

2. Approximation methods

2.1 Truncation approximation of the Voigt function

In the Abrarov algorithm II, the upper integration limit ∞ in Eq. (3) was replaced by $T = 12$ as sufficient for high-accuracy calculation since the exponential multiplier decays very rapidly with increasing t. Here we discuss the error caused by this truncation through numerical calculation in detail.

The truncation approximation of the VF is defined as

$$K_T(x,y) = \frac{1}{\sqrt{\pi}} \int_0^T \exp\left(-\frac{t^2}{4}\right) \exp(-yt) \cos(xt) dt, \tag{4}$$

(where T is a real number), with a relative error given by

$$\Delta_T = \left| \frac{K_T(x,y) - K(x,y)}{K(x,y)} \right|. \tag{5}$$

Fig. 1 show the logarithm relative error $\log_{10}\Delta_T$ of the truncation approximation in the domain $0 \le x \le 15$ and $10^{-10} \le y \le 15$ (this domain is the most difficult for rapid and accurate computation of the VF, Ref[10]) at $T = 10$, 12, 14, and 16 respectively.

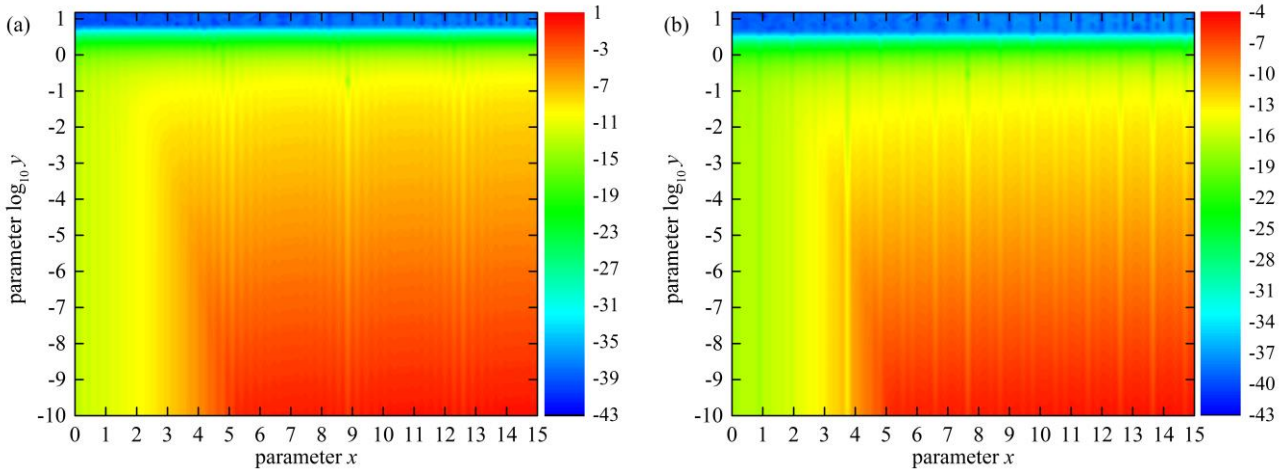

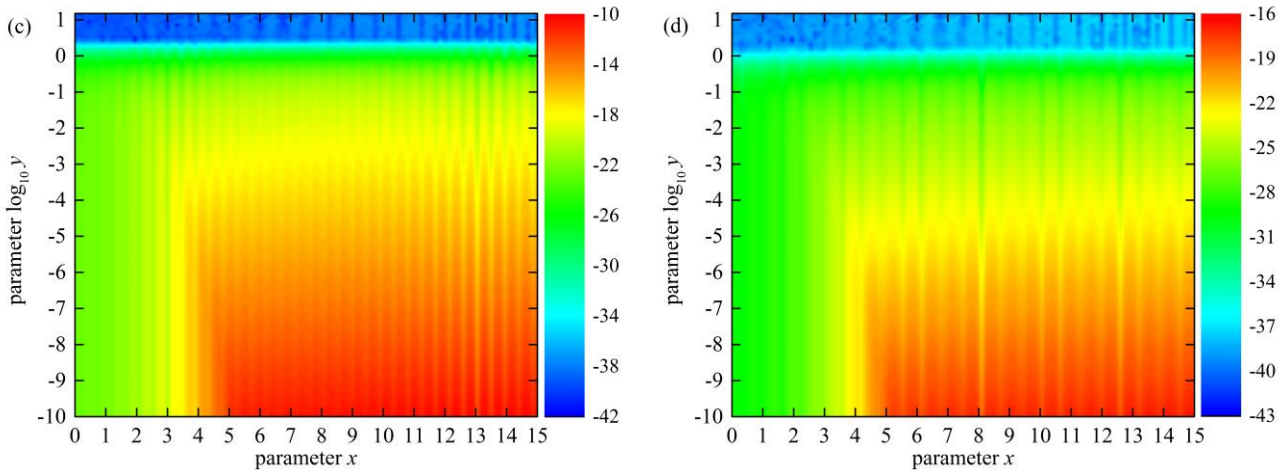

Fig. 1. Contour plot of $\log_{10}\Delta_T$ for domain $0 \le x \le 15$ and $10^{-10} \le y \le 15$ at (a) $T = 10$, (b) $T = 12$, (c) $T = 14$ and (d) $T = 16$ respectively. The parameter y is using logarithmic axes.

As we can see from Fig. 1a, the relative error of the truncation approximation is less than 10^{-5} in the region $y \ge 10^{-4}$ and the relative error increases rapidly to 0.25 with decreasing y at $T = 10$. Figs. 1b, 1c and 1d illustrate that the maximum relative error is decreases significantly with the increase of T. For example, the maximum relative error still less than 10^{-17} even if y is very small ($y \ge 10^{-10}$) at $T = 16$.

2.2 Approximation of exponential multiplier in arbitrary interval

The exponential multiplier $\exp(-1/4t^2)$ can be approximated by Fourier series within a certain integration domain $[-\tau, \tau]$ as

$$\exp(-\frac{t^2}{4}) \approx \sum_{n=0}^{N} a_n \cos(\frac{\pi n}{\tau} t), \tag{6}$$

with a relative error given by

$$\delta(t) = \left| [\exp(-t^2/4) - \sum_{n=0}^{N} a_n \cos(\frac{\pi n}{\tau} t)] / \exp(-t^2/4) \right|, \tag{7}$$

where the corresponding expansion coefficients are

$$a_n = \frac{1}{(1+\delta_{n0})\tau} \int_{-\tau}^{\tau} \exp(-\frac{1}{2}t^2) \cos(\frac{n\pi}{\tau} t) dt. \tag{8}$$

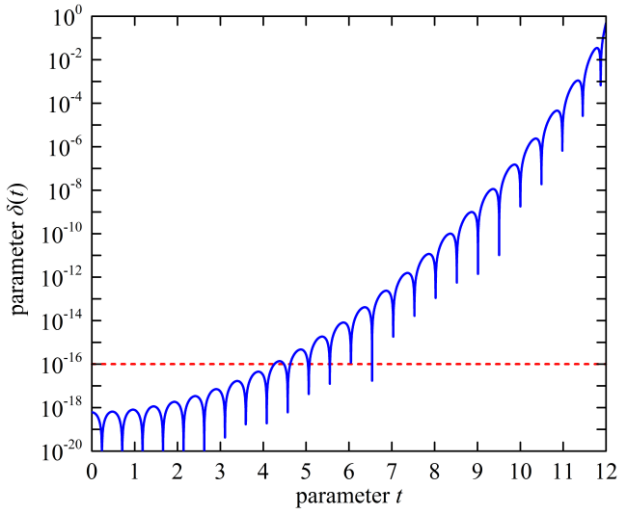

Fig. 2.

Fig. 2 The relative error $\delta(t)$ at $N = 23$ within the integration domain $t \in [0, \tau]$, where $\tau = 12$.

Fig. 2 illustrates the relative error δ(t) at $N = 23$ within the integration domain $t \in [0, \tau]$, where $\tau = 12$. As we can see the accuracy of Eq. (6) is better than 10^{-16} in the smaller domain $t \in [0, 4]$, however the accuracy deteriorates further with decreasing y. This fact explains that the accuracy of Abrarov algorithm I is two orders lower than the truncation approximation ($T = 12$) of the VF.

In order to achieve the high accuracy of the exponential multiplier in a larger interval, the number of terms of Eq. (6) needs to be greatly increased, which will significantly reduce the computational efficiency of VF. In this work, piecewise function method is used to approximate the exponential multiplier in arbitrary interval with high accuracy as following

$$\begin{aligned} \exp(-\frac{t^2}{4}) &= \exp[\frac{(2m+1)^2 T_0^2}{4}]\exp[-\frac{(2m+1)T_0 t}{2}]\exp[-\frac{(t-(2m+1)T_0)^2}{4}] \\ &\approx \exp[\frac{(2m+1)^2 T_0^2}{4}]\exp[-\frac{(2m+1)T_0 t}{2}]\sum_{n=0}^{N} a_n \cos[\frac{\pi n}{\tau}(t-(2m+1)T_0)] \qquad 2mT_0 \le t < 2(m+1)T_0, m = 0,1,..., \end{aligned} \tag{9}$$

where T_0 is smaller than τ to ensure higher accuracy of exponential multiplier. The accuracy of Eq. (9) is determined by the maximum relative error of Eq. (6) in the subdomain $t \in [0, T_0]$, for example, the maximum relative error of Eq. (9) is less than 10^{-16} in arbitrary interval while $N = 23$, $\tau = 12$ and $T_0 = 4$.

2.3 Approximations expressions of Voigt function

By substituting Eq. (9) into Eq. (3), the following approximations expressions of VF in analytic form is yielded (Appendix A)

$$K_P(x,y) = \sum_{m=0}^{M} \frac{1}{2\sqrt{\pi}} \exp[-y(2m+1)T_0 - \frac{(2m+1)^2 T_0^2}{4}] I_m(x,y), \tag{10}$$

where $2MT_0$ is the upper integration limit of the truncation approximation of the VF, and

$$\begin{aligned} I_m = \sum_{n=0}^{N} a_n \Bigg[& \frac{e^{\alpha_m T_0}}{\alpha_m^2 + \beta_{n+}^2} \left(\alpha_m \cos(\beta_{n+} T_0 + \gamma_m) + \beta_{n+} \sin(\beta_{n+} T_0 + \gamma_m)\right) \\ & - \frac{e^{-\alpha_m T_0}}{\alpha_m^2 + \beta_{n+}^2} \left(\alpha_m \cos(-\beta_{n+} T_0 + \gamma_m) + \beta_{n+} \sin(-\beta_{n+} T_0 + \gamma_m)\right) \\ & + \frac{e^{\alpha_m T_0}}{\alpha_m^2 + \beta_{n-}^2} \left(\alpha_m \cos(\beta_{n-} T_0 + \gamma_m) + \beta_{n-} \sin(\beta_{n-} T_0 + \gamma_m)\right) \\ & - \frac{e^{-\alpha_m T_0}}{\alpha_m^2 + \beta_{n+}^2} \left(\alpha_m \cos(-\beta_{n-} T_0 + \gamma_m) + \beta_{n-} \sin(-\beta_{n-} T_0 + \gamma_m)\right) \Bigg], \end{aligned} \tag{11}$$

and the coefficients in Eq.(11) is defined as follows

$$\begin{aligned} \alpha_m &= -y - \frac{(2m+1)T_0}{2}, \\ \beta_{n+} &= x + \frac{\pi n}{\tau}, \\ \beta_{n-} &= x - \frac{\pi n}{\tau}, \\ \gamma_m &= (2m+1)T_0 x. \end{aligned} \tag{12}$$

3. Results and discussion

3.1 Error Analysis

In order to quantify accuracy of the series approximation (10), it is convenient to define the relative error as

$$\Delta_p = \left| \frac{K_p(x,y) - K(x,y)}{K(x,y)} \right|, \tag{13}$$

where the highly accurate reference values of $K(x, y)$ can be obtained according to Eq. (1) by using the MATLAB that supports error function of complex argument.

Figures 3a and 3b show the logarithm $\log_{10}\Delta_P$ of the relative error of the series approximation (10) at N=33, M = 1, T_0 = 4.1515, and τ =14.3417 (the corresponding expansion coefficients a_n with 32-bit significant number are shown in Appendix B). The domain required for coverage of the HITRAN molecular spectroscopic database is $0 < x < 40{,}000$ and $10^{-4} < y < 10^{2}$[16] while the domain $y << 1$ is the most difficult for accurate and rapid computation of the Voigt function. Therefore, we will consider the accuracy behavior within the HITRAN domain and narrow band domain $10^{-4} \le x \le 40{,}000 \cap 10^{-4} \le y \le 10^{2}$ and $10^{-4} \le x \le 40{,}000 \cap 10^{-10} \le y \le 10^{-4}$ separately as shown in Figs. 2a and 2b, respectively.

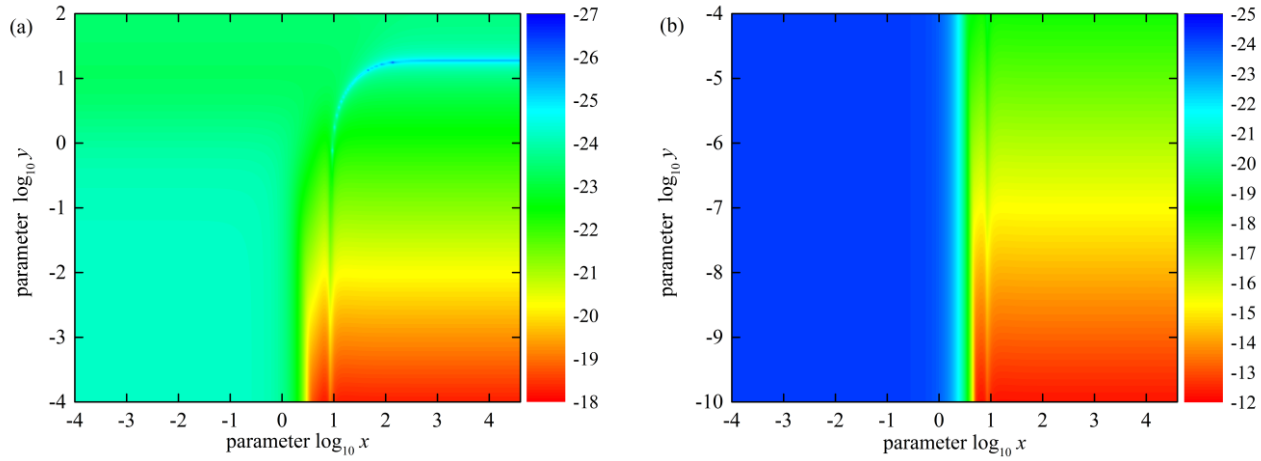

Fig. 3. Logarithms of the relative error $\log_{10}\Delta_P$: (a) for the HITRAN domain $10^{-4} \le x \le 40{,}000 \cap 10^{-4} \le y \le 10^{2}$ and b) for the narrow band domain $10^{-4} \le x \le 40{,}000 \cap 10^{-10} \le y \le 10^{-4}$. The parameters applied in computation are N = 33, M = 1, T_0 = 4.1515, and τ = 14.3417.

As we can see from Fig. 3a, within the HITRAN domain the accuracy of the series approximation is better than 10^{-23} over most of this area. The worst accuracies occurs in the HITRAN subdomain $3 \le x \le 40{,}000 \cap 10^{-4} \le y \le 10^{-2}$, and remains high and better than 5.5383×10^{-19}. In the narrow band shown in the Fig. 2b, the accuracy deteriorates further with decreasing y. However, it still remains high and better than 10^{-15} over most of this area. The worst accuracies occurs in the narrow band subdomain $3 \le x \le 40{,}000 \cap 10^{-10} \le y \le 10^{-8}$, and remains high and better than 5.5385×10^{-13}. The increase of $\log_{10}\Delta_P$ can be explained from the fact that the decay rate of the multiplier $\exp(-yt)$ in Eq. (3) decelerates when $y \to 0$.

3.2 Parameter optimization

Since higher accuracy is unnecessary in some cases, for example, the accuracy of the Voigt function should be better than 10^{-6} in modern applications requiring the HITRAN molecular spectroscopic database, we may select the optimal parameters to minimize the number of terms in the series approximation (10) in order to gain computational acceleration. By numerical calculation, the optimal parameters under different accuracy levels are shown in Table 1.

Table 1. The optimal parameters N, M, T_0, and τ under different accuracy levels Δ.

N	M	T_0	τ	$(M+1)\times N$	Δ^a
7	1	2.4716	6.6882	14	3.1334×10^{-2}

9	1	2.5397	7.5067	18	2.2091×10^{-3}
11	1	3.9996	8.2866	22	7.1448×10^{-4}
13	1	3.0487	8.9895	26	4.5214×10^{-6}
15	1	3.5094	9.6666	30	4.0066×10^{-7}
17	1	3.3199	10.2881	34	1.1289×10^{-8}
19	1	3.7118	10.8779	38	9.9817×10^{-10}
21	1	4.0616	11.4342	42	8.7514×10^{-11}
23	1	3.9064	11.9687	46	2.5609×10^{-12}
25	1	3.5211	12.4853	50	9.2548×10^{-14}
27	1	4.0921	12.9691	54	6.6239×10^{-15}
29	1	3.9683	13.4438	58	2.1007×10^{-16}
31	1	3.8627	13.9084	62	7.7856×10^{-18}
33	1	4.1515	14.3417	66	5.5383×10^{-19}

[a] Δ represents the worst accuracy within the HITRAN domain $0 < x < 40{,}000$ and $10^{-4} \le y \le 10^{2}$.

4. Conclusion

A analytical approximation expressions for rapid and accurate computation of the Voigt function is presented. The computational test reveals that with only the first 33 terms Fourier expansion of the exponential multiplier, the proposed approximation provides accuracy better than 5.5383×10^{-19} in the domain of practical interest $0 < x < 40{,}000$ and $10^{-4} < y < 10^{2}$ that is needed for applications using the HITRAN molecular spectroscopic database. Compared with the typical approximation algorithms, the proposed approximation still available even if y is very small and the accuracy in the narrow band domain $0 < x < 40{,}000 \cap 10^{-10} < y < 10^{-4}$ remains high and better than 5.5385×10^{-13}. Since the approximations Eq. (10) is a general expressions, the desired accuracy can be easily achieved by choosing reasonable parameters. In particular, the optimal parameters under different accuracy levels from 10^{-2} to 10^{-19} are given in Table 1 in order to gain computational acceleration.

Appendix A

The infinite integral interval in Eq. (3) can be rewritten in the following form

$$K(x,y)=\sum_{m=0}^{\infty}\frac{1}{\sqrt{\pi}}K_m(x,y), \tag{A-1}$$

where $K_m(x,y)$ is defined as

$$K_m(x,y)=\int_{2mT_0}^{2(m+1)T_0}\exp(-\frac{t^2}{4})\exp(-yt)\cos(xt)dt. \tag{A-2}$$

By substituting Eq. (9) into Eq. (A-2) and using the product to sum formulas for cosine functions, the $K_m(x,y)$ can be approximated in the following form

$$K_m(x,y)\approx\frac{1}{2}\exp[-y((2m+1)T_0)-\frac{(2m+1)^2T_0^2}{4}]\sum_{n=0}^{N}a_n[I_{mn1}(x,y)+I_{mn2}(x,y)], \tag{A-3}$$

where $I_{mn1}(x,y)$ and $I_{mn2}(x,y)$ are defined as

$$I_{mn1}(x,y)=\int_{-T_0}^{T_0}\exp[-(y+\frac{2(2m+1)T_0}{4})t]\cos[(x+\frac{\pi n}{\tau_m})t+(2m+1)xT_0]dt, \tag{A-4}$$

$$I_{mn2}(x,y)=\int_{-T_0}^{T_0}\exp[-(y+\frac{2(2m+1)T_0}{4})t]\cos[(x-\frac{\pi n}{\tau_m})t+(2m+1)xT_0]dt. \quad \text{(A-5)}$$

The exact solutions of integral (A-4) and (A-5) can be found analytically by using the following formula

$$\int e^{ax}\cos bxdx=e^{ax}\frac{a\cos bx+b\sin bx}{a^2+b^2}, \quad \text{(A-4)}$$

$$\int e^{ax}\sin bxdx=e^{ax}\frac{a\sin bx-b\cos bx}{a^2+b^2}. \quad \text{(A-5)}$$

Thus the approximations expressions of VF in analytic form is yielded by taking the first M terms of Eq. (A-1).

Appendix B

Table B-1. The corresponding expansion coefficients a_n with 32-bit significant number (τ =14.3417).

a_n	values	a_n	values
a_0	0.12358749684139805606487391160845	a_{17}	2.34663226509694125264896819695 96×10^{-7}
a_1	0.23559454230112804343225836792199	a_{18}	4.37591946368976855350794485437 68×10^{-7}
a_2	0.20400805103788656794943165547129	a_{19}	7.41335829942177526106090636143 42×10^{-9}
a_3	0.16049103428021140229749175377995	a_{20}	1.14099055312638726321578152123 39×10^{-9}
a_4	0.11470322597572434645667951846306	a_{21}	1.59540332987922930328540195226 34×10^{-10}
a_5	7.44769488929174963631564872424 15×10^{-2}	a_{22}	2.02665734605729322700028769505 48×10^{-11}
a_6	4.39328632154471663818634115164 02×10^{-2}	a_{23}	2.33889942917443778395581776070 27×10^{-12}
a_7	2.35439066721185507609636615035 04×10^{-2}	a_{24}	2.45224668507766323684321163079 42×10^{-13}
a_8	1.14627530034699272490627379415 5×10^{-2}	a_{25}	2.33581343451475663611454678218 71×10^{-14}
a_9	5.07014907559382370130513693235 5×10^{-3}	a_{26}	2.02131284219685805124508429806 52×10^{-15}
a_{10}	2.03738878383534272613955221715 92×10^{-3}	a_{27}	1.58909663437597113635331745855 8×10^{-16}
a_{11}	7.43786823886321146779972487281 08×10^{-4}	a_{28}	1.13498061717862579672680786097 95×10^{-17}
a_{12}	2.46685962996627130981033904108 23×10^{-4}	a_{29}	7.36458555154868663598872872309 87×10^{-19}
a_{13}	7.43295977677967410909490634026 54×10^{-5}	a_{30}	4.34134199513665075719311389965 73×10^{-20}
a_{14}	2.03470060881429559915468145262 66×10^{-5}	a_{31}	2.32552412134584317658959567055 23×10^{-21}
a_{15}	5.06011788900624112297148317910 24×10^{-6}	a_{32}	1.12658751724348346034527346235 74×10^{-22}
a_{16}	1.14325245480222568339105896113 6×10^{-6}	a_{33}	5.45172710642973570380989572397 28×10^{-24}

Reference

[1] Mendonca J, Strong K, Sung K, et al. Using high-resolution laboratory and ground-based solar spectra to assess CH 4 absorption coefficient calculations[J]. Journal of Quantitative Spectroscopy & Radiative Transfer, 2017, 190:48-59.

[2] Loos J , Birk M , Wagner G . Measurement of positions, intensities and self-broadening line shape parameters of H 2O lines in the spectral ranges 1850–2280 cm $^{-1}$, and 2390–4000 cm^{-1}[J]. Journal of Quantitative Spectroscopy & Radiative Transfer, 2017:S0022407317300419.

[3] Dong C , Boqiang F , Ying H E , et al. Laser absorption spectroscopy data processing method based on

co-frequency and dual-wavelength and its application[J]. Optics Express, 2018, 26:4459-4469.

[4] Al-Jalali M A , Aljghami I F , Mahzia Y M . Voigt deconvolution method and its applications to pure oxygen absorption spectrum at 1270nm band[J]. Spectrochimica Acta Part A: Molecular and Biomolecular Spectroscopy, 2016, 157:34-40.

[5] Armstrong BH, Nicholls RW. Emission, absorption and transfer of radiation in heated atmospheres. New York: Pergamon Press;1972.

[6] J. Humlicek. Optimized computation of the voigt and complex probability functions[J]. Journal of Quantitative Spectroscopy and Radiative Transfer, 1982, 27(4):437-444.

[7] WELLS R. J. Rapid approximation to the Voigt/Faddeeva function and its derivatives[J]. Journal of Quantitative Spectroscopy & Radiative Transfer, 1999, 62(1):29-48.

[8] Abrarov S M , Quine B M , Jagpal R K . Rapidly convergent series for high-accuracy calculation of the Voigt function[J]. Journal of Quantitative Spectroscopy and Radiative Transfer, 2010, 111(3):372-375.

[9] Abrarov S M , Quine B M , Jagpal R K . High-accuracy approximation of the complex probability function by Fourier expansion of exponential multiplier[J]. Computer Physics Communications, 2010, 181(5):876-882.

[10] Abrarov S M , Quine B M . A Rational Approximation for Efficient Computation of the Voigt Function in Quantitative Spectroscopy[J]. Journal of Mathematics Research, 2015, 7(2).

[11] Abrarov, S. M., & Quine, B. M. (2014). Master-Slave Algorithm for Highly Accurate and Rapid Computation of the Voigt/Complex Error Function. Journal of Mathematics Research, 2014,6:104-119.

[12] Weideman J A C . Computations of the complex error function[M]. Society for Industrial and Applied Mathematics, 1994.

[13] Abrarov S M , Quine B M . Efficient algorithmic implementation of the Voigt/complex error function based on exponential series approximation[J]. Applied Mathematics & Computation, 2011, 218(5):1894-1902.

[14] Abrarov S M , Quine B M . Accurate approximations for the complex error function with small imaginary argument[J]. Journal of Mathematics Research, 2014, 7(1).

[15] Amamou H, Ferhat B, Bois A. Calculation of the Voigt function in the region of very small values of the parameter a where the calculation is notoriously difficult[J]. American Journal of Analytical Chemistry, 2013, 4(12): 725.

[16] Gordon I E, Rothman L S, Hill C, et al. The HITRAN2016 molecular spectroscopic database[J]. Journal of Quantitative Spectroscopy and Radiative Transfer, 2017, 203: 3-69.